GENERIC SPECTRUM AND IONIZATION EFFICIENCY OF A HEAVY INITIAL MASS FUNCTION FOR THE FIRST STARS

VOLKER BROMM

Department of Astronomy, Yale University, New Haven, CT 06520-8101; volker@astro.yale.edu

ROLF P. KUDRITZKI

Institute for Astronomy, University of Hawaii, 2680 Woodlawn Drive, Honolulu, HI 96822; kud@ifa.hawaii.edu

AND

ABRAHAM LOEB

Astronomy Department, Harvard University, 60 Garden Street, Cambridge, MA 02138; aloeb@cfa.harvard.edu

ABSTRACT

We calculate the generic spectral signature of an early population of massive stars at high redshifts. For metal-free stars with mass above 300 $M_\odot$, we find that the combined spectral luminosity per unit stellar mass is almost independent of the mass distribution of these stars. To zeroth order, the generic spectrum resembles a blackbody with an effective temperature of $\sim 10^5$ K, making these stars highly efficient at ionizing hydrogen and helium. The production rate of ionizing radiation per stellar mass by stars more massive than ~ 300 $M_\odot$ is larger by ~ 1 order of magnitude for hydrogen and He I and by ~ 2 orders of magnitude for He II than the emission from a standard initial mass function. This would result in unusually strong hydrogen and helium recombination lines from the surrounding interstellar medium. It could also alleviate the current difficulty of ionizing the intergalactic medium at $z \gtrsim 6$ with the cosmic star formation rate inferred at somewhat lower redshifts.

Subject headings: cosmology: theory — early universe — intergalactic medium — stars: atmospheres — stars: formation — ultraviolet: stars

1. INTRODUCTION

One of the most important challenges in modern cosmology is to understand when and how the cosmic "dark ages" ended (Loeb 1998, 1999; Rees 1999). The absence of a Gunn-Peterson trough in the spectra of high-redshift quasars implies that the universe was reionized at a redshift $z > 5.8$ (Fan et al. 2000). An early, pregalactic generation of stars (the so-called Population III) has long been suspected to control this process (e.g., Carr, Bond, & Arnett 1984; Couchman & Rees 1986; Haiman & Loeb 1997). The feedback of the first generation of stars on the ionization history of the intergalactic medium (IGM) depends crucially on their initial mass function (IMF). Recent numerical simulations presented evidence that the primordial IMF might have favored massive stars with a mass $\gtrsim 10^2$ $M_\odot$ (Bromm, Coppi, & Larson 1999, 2001; Abel, Bryan, & Norman 2000). This prediction relies on the existence of a characteristic scale for the density and temperature of the primordial gas and consequently of a characteristic Jeans mass of $M_J \sim 10^3$ $M_\odot$ (see also Larson 1998). At present, it is not known with any certainty what fraction of a Jeans-unstable clump of gas will eventually be incorporated into the resulting star. This is due to the complicated physics of the protostellar feedback on a dust-free envelope and the accretion from it.

Here we adopt the view that the simulated clump masses are indicative of the final stellar masses and explore the implications. Recent observations of the formation process of present-day stars seem to support this view. Motte, André, & Neri (1998) have mapped the nearby ρ Ophiuchi star-forming cloud in the 1.3 mm dust continuum. Their study identifies a number of dense, gravitationally bound clumps with masses close to stellar values, which appear to lack the emission from embedded stellar sources. These

starless clumps, therefore, might be the direct progenitors of individual stars.

Ultimately, the question of how massive the first stars were has to be answered by observations. It is therefore important to ask whether future observatories, such as the *Next Generation Space Telescope* (*NGST*), could place any constraints on the primordial IMF. To address this question, we have constructed models for the interior structure and the emerging spectra of massive Population III stars. Since metal-free stars have systematically higher effective temperatures ($T_{\rm eff} \sim 10^5$ K for $M > 100$ $M_\odot$), they are very efficient at producing photons capable of ionizing hydrogen and helium. The reionization of the intergalactic helium has traditionally been attributed to a population of quasars. A generation of very massive Population III stars would provide an important alternative channel, operating at redshifts higher than what is typically assumed for quasars.

Recently, Tumlinson & Shull (2000) have discussed the case of metal-free stars with a normal (Salpeter-like) IMF, up to masses of 90 $M_\odot$ (see also Ciardi et al. 2000b for the effect of introducing a lower mass cutoff at $M_c = 5$ $M_\odot$). It is important, however, to extend this mass range into the regime of very massive stars with $M > 100$ $M_\odot$, since both the nature of the feedback on the IGM and the spectral characteristics change in a significant way for this regime.

In § 2 we describe our models for the stellar interior and for the spectrum. In §§ 3 and 4 we address the ionization efficiency and discuss the observational signatures, respectively. Finally, in § 5 we summarize the implications of our results.

2. STELLAR MODELS

2.1. *Stellar Structure*

We construct models for static, metal-free stars in com-

plete (i.e., dynamical and thermal) equilibrium by solving the time-independent equations of stellar structure (e.g., Schwarzschild 1958; Kippenhahn & Weigert 1990). The integration is performed in the standard way by fitting solutions for the core and envelope at a suitably chosen intermediate point, and the considered mass range is $100 \leq M/M_\odot \leq 1000$. Stars in this mass range have traditionally been termed very massive objects (VMOs; Bond, Arnett, & Carr 1984). For such a massive star with the concomitant high interior temperatures, the only effective source of opacity is electron scattering, given by $\kappa = 0.2(1 + X)$ cm^2 g^{-1}, where $X \simeq 0.76$ is the mass fraction in hydrogen. Other sources of opacity are not included in our calculations.

In the absence of metals and, in particular, of the catalysts necessary for the operation of the CNO cycle, nuclear burning proceeds in a nonstandard way. At first, hydrogen burning can only occur via the inefficient p-p chain. To provide the necessary luminosity, the star has to reach very high central temperatures ($T_c \simeq 10^{8.1}$ K). These temperatures are high enough for the simultaneous occurrence of helium burning via the triple-α process. After a brief initial period of triple-α burning, a trace amount of heavy elements has been formed. Subsequently, the star follows the CNO cycle. In constructing our main-sequence models, we therefore assume a level of pre-enrichment with metals, amounting to a mass fraction of $Z = 10^{-9}$. The resulting models consist of a convective core, containing 90%–100% of the mass, and a thin radiative envelope. As a result of the high mass and temperature, the stars are dominated by radiation pressure and have luminosities close to the Eddington limit: $L \simeq L_{\rm Edd} = 1.25 \times 10^{38}$ ergs s^{-1} $(M/M_\odot)$.

In this paper we do not include the evolution of the stars away from the main sequence, which crucially depends on the poorly understood mass-loss mechanism. While this is clearly an idealization, it is justified by the fact that the stars spend a major fraction of their total lifetime, estimated to be $\tau \simeq 0.007Mc^2/L_{\rm Edd} \sim 3 \times 10^6$ yr, near the location of the main sequence.

In Figure 1 we show the resulting sequence of models for Population III stars and compare to the corresponding Population I sequence (calculated with $Z = 0.02$). Our results agree well with those of El Eid, Fricke, & Ober (1983) in the mass range $100 < M/M_\odot < 500$. It is evident that the respective effective temperatures approach an asymptotic value that is independent of mass, $T_{\rm eff} \simeq 1.1 \times 10^5$ K for Population III and $T_{\rm eff} \simeq 6.5 \times 10^4$ K for Population I. This characteristic behavior of very massive stars derives from the assumptions of hydrostatic equilibrium, radiation pressure support with a luminosity close to the Eddington limit, and the nuclear physics of hydrogen burning. The peculiar behavior of very massive Population III stars has already been discussed by a number of previous authors (see Bond, Arnett, & Carr 1984 and references therein). Bond, Arnett, & Carr (1984), in particular, have pointed out that the effective temperature, $T_{\rm eff} \sim 10^5$ K, is almost independent of mass for $M > 100\ M_\odot$. For completeness, we here give a somewhat simplified version of the argument.

The mechanical structure of a massive, radiation pressure–dominated star is approximately given by a polytrope of index $n = 3$ (see Kippenhahn & Weigert 1990). If $w(z)$ is the corresponding solution of the Lane-Emden equation and $z = (z_3/R)r$ the dimensionless radial coordinate,

one can express the density and pressure as $\rho = \rho_c w^3$ and $P = (\pi G R^2 \rho_c^{2/3}/z_3^2)\rho^{4/3}$, respectively. Here $z_3 = 6.89685$ is the dimensionless radius of the polytrope, $\rho_c = 54.1825(3M/4\pi R^3)$ is the central density, and the other symbols have their usual meaning. With the polytropic value for the central pressure, $P_c \simeq 11.1GM^2/R^4$, one can estimate the temperature at the center of the star, $T_c = (3P_c/a)^{1/4}$, to be

$$T_c \simeq (8.4 \times 10^7 \text{ K})\left(\frac{M}{100\ M_\odot}\right)^{1/2}\left(\frac{R}{10\ R_\odot}\right)^{-1}. \quad (1)$$

To constrain T_c further, we follow Fowler & Hoyle (1964) and consider the global energy balance of the star. The average nuclear energy generation rate (in ergs s^{-1} g^{-1}) is $\bar{\epsilon} = L/M = \int_0^M \epsilon\, dm$, and we assume $\epsilon \simeq \epsilon_{\rm CNO}$. Writing $\epsilon = \epsilon_c(\rho/\rho_c)(T/T_c)^\nu$, with c denoting central values, one finds

$$\bar{\epsilon} \simeq 162.5\epsilon_c\left(\frac{1}{z_3^3}\int_0^{z_3} w^{6+\nu}z^2\, dz\right). \quad (2)$$

A reasonable fit to the CNO cycle energy generation rate close to $\log T \simeq 8.1$ is given by

$$\epsilon \simeq 1.3 \times 10^{12} ZX\rho\left(\frac{T}{10^8\text{ K}}\right)^8. \quad (3)$$

This form derives from a linear fit to the exact expression for $\epsilon_{\rm CNO}$ (Kippenhahn & Weigert 1990), at $\log T \simeq 8.1$. Using $\nu = 8$ in equation (2) gives $\bar{\epsilon} \simeq 0.05\epsilon_c$. From $L \simeq L_{\rm Edd} = \bar{\epsilon}M$ follows the desired relation

$$T_c \simeq (1.9 \times 10^8 \text{ K})\left(\frac{Z}{10^{-9}}\right)^{-1/8}\left(\frac{M}{100\ M_\odot}\right)^{-1/8}\left(\frac{R}{10\ R_\odot}\right)^{3/8}. \quad (4)$$

Combining equations (1) and (4) gives the mass-radius relation for very massive stars

$$M \simeq (370\ M_\odot)\left(\frac{Z}{10^{-9}}\right)^{-0.2}\left(\frac{R}{10\ R_\odot}\right)^{2.2}, \quad (5)$$

from which it can be seen that approximately $M \propto R^2$. Finally, the effective temperature can be estimated from $L \simeq L_{\rm Edd} = 4\pi R^2 \sigma T_{\rm eff}^4$. Using equation (5) to eliminate the radius, we find

$$T_{\rm eff} \simeq (1.1 \times 10^5 \text{ K})\left(\frac{Z}{10^{-9}}\right)^{-0.05}\left(\frac{M}{100\ M_\odot}\right)^{0.025}. \quad (6)$$

This analytical estimate for $T_{\rm eff}$ and the very weak dependence on mass are in good agreement with the numerical results in Figure 1.

2.2. Emergent Spectrum

Having determined the basic stellar parameters, we now construct model atmospheres and emergent spectra. The extreme luminosities very close to the Eddington limit and the very high effective temperatures require the sophisticated effort of using non-LTE (NLTE) unified model atmospheres with spherical extension and stellar winds, as originally introduced by Gabler et al. (1989). This new type of model atmosphere provides a smooth transition from the
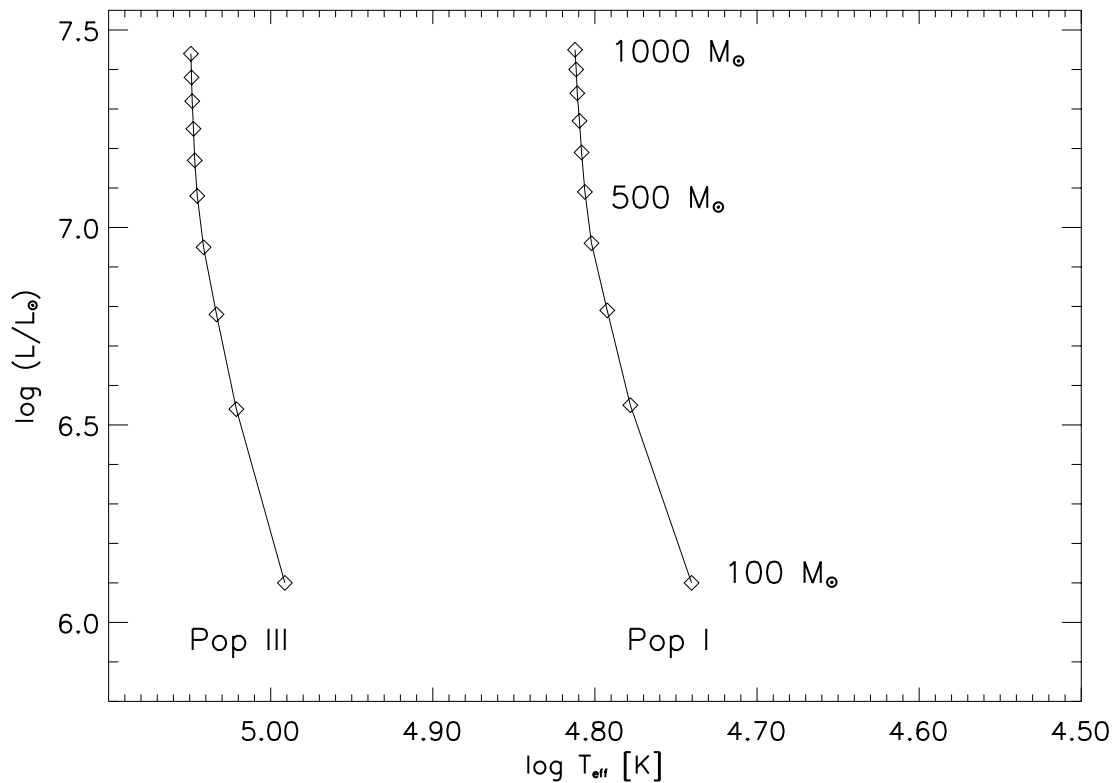
FIG. 1.—Zero-age main sequence (ZAMS) of very massive stars. *Left solid line:* Population III ZAMS. *Right solid line:* Population I ZAMS. In each case, stellar luminosity (in $L_\odot$) is plotted vs. effective temperature (in K). *Diamonds:* Stellar masses along the sequence, from 100 $M_\odot$ (*bottom*) to 1000 $M_\odot$ (*top*) in increments of 100 $M_\odot$. The Population III ZAMS is systematically shifted to higher effective temperature, with a value of $\sim 10^5$ K, which is approximately independent of mass. The luminosities, on the other hand, are almost identical in the two cases.

subsonic, quasi-hydrostatic photosphere to the supersonic, radiation-driven stellar wind and allows the simultaneous treatment of spectral features formed deep in the photosphere (such as optical continua and line wings) and those arising from the outer layers, where the influence of winds becomes significant (such as strong absorption edges, far-infrared continua, and line cores). A detailed discussion is given by Kudritzki (1998).

For this paper we use the new unified model code originally developed by Santolaya-Rey, Puls, & Herrero (1997) and further improved by J. Puls (2000, private communication). Bound-bound, bound-free, and free-free absorption by hydrogen and helium and Thomson scattering are included as opacity sources. A value of 0.1 has been adopted for the number ratio of helium to hydrogen. Changing this ratio toward slightly smaller values closer to estimates for the primordial helium abundance would not lead to a significant modification of the calculated spectra.

The atmospheric models are fully specified by the effective temperature, the gravity, and the stellar radius (all taken at the Rosseland optical depth $\tau_{\rm Ross} = \frac{2}{3}$) together with the mass-loss rate $\dot{M}$, the terminal velocity v_∞, and the parameter β, which describes the radial slope of the velocity field via

$$v(r) = v_\infty \left(1 - \frac{b}{r}\right)^\beta. \tag{7}$$

The constant b is chosen to guarantee a smooth transition into the hydrostatic stratification at a prespecified outflow velocity smaller than the isothermal sound speed (normally

$0.1c_s$). Velocity fields of this form are predicted by the theory of radiation-driven winds (e.g., Castor, Abbott, & Klein 1975; Pauldrach, Puls, & Kudritzki 1986) and usually lead to an excellent fit to observed stellar wind lines based on radiative transfer and model atmosphere calculations (see Kudritzki & Puls 2000).

At zero metallicity, we expect stellar winds to be of only minor importance. However, a radiation-driven wind might still arise as a result of the opacity in the He II resonance lines, in combination with the contribution from bound-free and free-free absorption. No wind models have been constructed so far for this extreme case of zero metallicity. Kudritzki (2000) has developed a new algorithm, which allows one to deal with line-driven winds at very low metallicity down to 10^{-4} of the solar value. As a rough extrapolation from his results, we adopt $\dot{M} = 10^{-10}\, M_\odot$ yr^{-1}, $v_\infty = 1900$ km s^{-1}, and $\beta = 1$. This choice of stellar wind parameters results in an almost hydrostatic, but still spherically extended, density structure. From a number of additional test calculations carried out with different wind parameters we note that the resulting emergent spectra show only a very small parameter dependence as long as the winds are weak. For instance, enhancing the mass-loss rate to a value of $\dot{M} = 10^{-8}\, M_\odot$ has little influence on the energy distribution and line profiles.

In Figure 2 we present the resulting spectra for different masses. Shown is the specific flux, F_ν, at the surface of the star. At these high effective temperatures, there is still a rich spectrum of He II and H lines in the EUV, UV, optical, and IR. Some of these lines show emission features as a result of an overpopulation of their upper levels due to NLTE
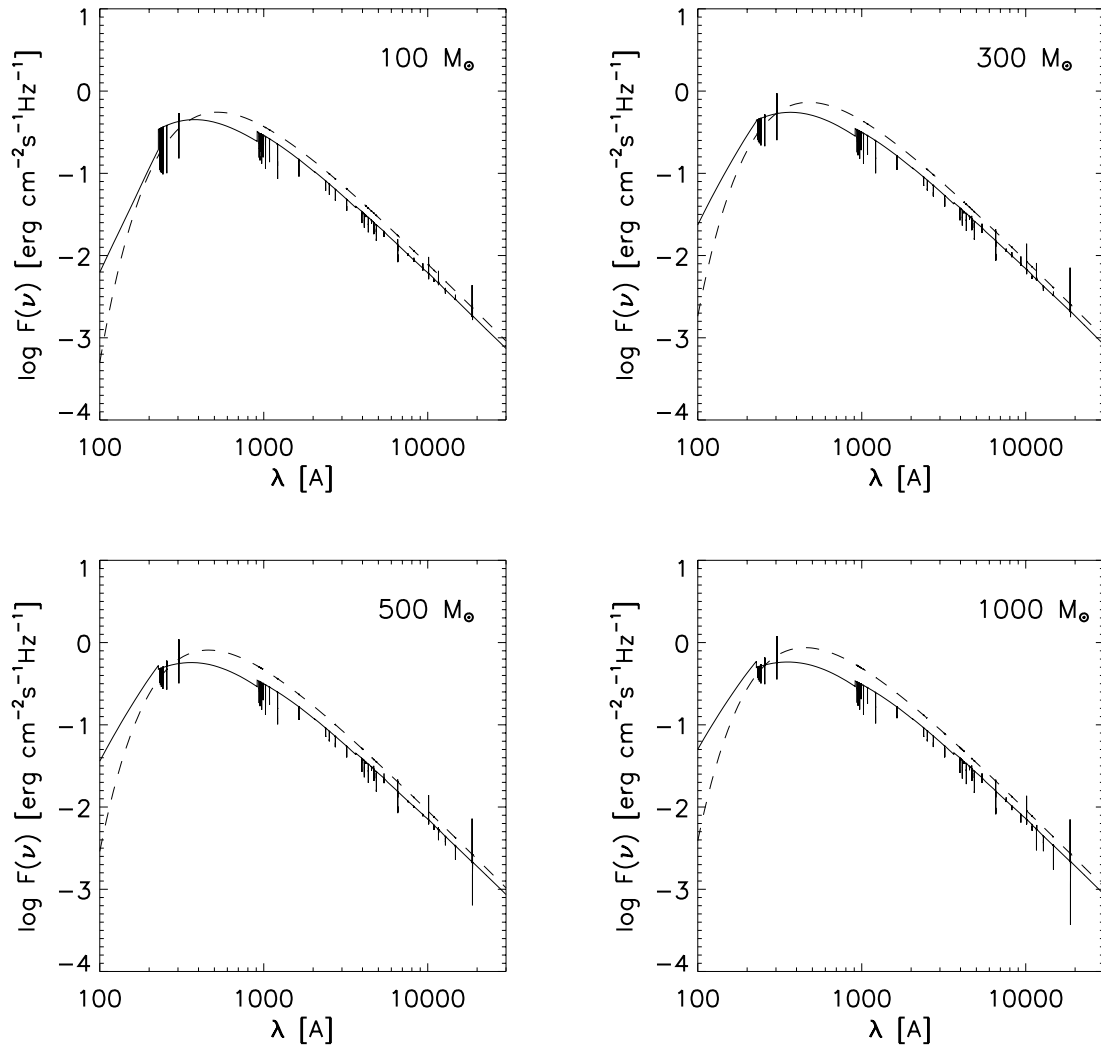
FIG. 2.—Spectra of very massive Population III stars. *Solid lines:* Flux at the surface of the star (in units of ergs s^{-1} cm^{-2} Hz^{-1}) vs. wavelength (in Å). *Dashed lines:* Corresponding blackbody spectrum, evaluated at the respective effective temperatures. Lines are due to transitions of H and He II in the EUV, UV, optical, and IR bands. The spectra for $M = 100, 300, 500,$ and 1000 $M_\odot$ are remarkably similar, differing only slightly in the strengths of the He II and H I ionization edges at 228 and 912 Å, respectively.

effects. The He II resonance lines have emission wings and central absorption cores, whereas some of the He II Pickering lines have a central emission peak on top of absorption wings. Such types of line profiles reflect the stratification of the ratio of the NLTE departure coefficients of the upper to the lower line level and are common for very hot stars. A first interpretation of the underlying physics has been given in the pioneering paper by Auer & Mihalas (1972). Strikingly, the He II absorption edge at 228 Å is very weak or turns into emission for higher masses. This is again a distinct NLTE effect, which has been discussed in detail by Husfeld et al. (1984) and Gabler et al. (1989, 1992).

For $M > 300$ $M_\odot$, the spectra become increasingly similar. This similarity is even more evident when the resulting specific luminosity, $L_\nu = 4\pi R^2 F_\nu$, is plotted per unit stellar mass, as shown in Figure 3. Stars with luminosities close to the Eddington limit, $L_\nu \propto L_{\rm Edd} \propto M$, approach a universal value for their flux per unit mass. The prediction that the total spectral luminosity depends only on the total mass of stars but is independent of the IMF is a unique feature of a population of very massive stars. In § 4 we explore the observational consequences of this result but

discuss first the production of ionizing photons from these stars.

3. FEEDBACK EFFECTS

The spectrum for a population of very massive, zero-metallicity stars deviates most strongly from the case with a Salpeter IMF at short wavelengths, near the peak of the corresponding blackbody at $\lambda_{\rm em} \simeq 250$ Å. An important difference is therefore expected in the rate of producing ionizing photons. To quantify this effect for the species H I, He I, and He II, we calculate the number of ionizing photons per unit stellar mass according to

$$\dot{N}_{\rm ion} = \frac{1}{M} \int_{\nu_{\rm th}}^{\infty} \frac{L_\nu \, d\nu}{h\nu}, \tag{8}$$

where $\nu_{\rm th}$ is the respective threshold for ionization. We here make the somewhat idealized assumption that all Population III stars were more massive than 300 $M_\odot$. Therefore, as demonstrated in the previous section, their spectra, when scaled to stellar mass, have a generic form that is almost independent of mass. Specifically, we take the luminosity
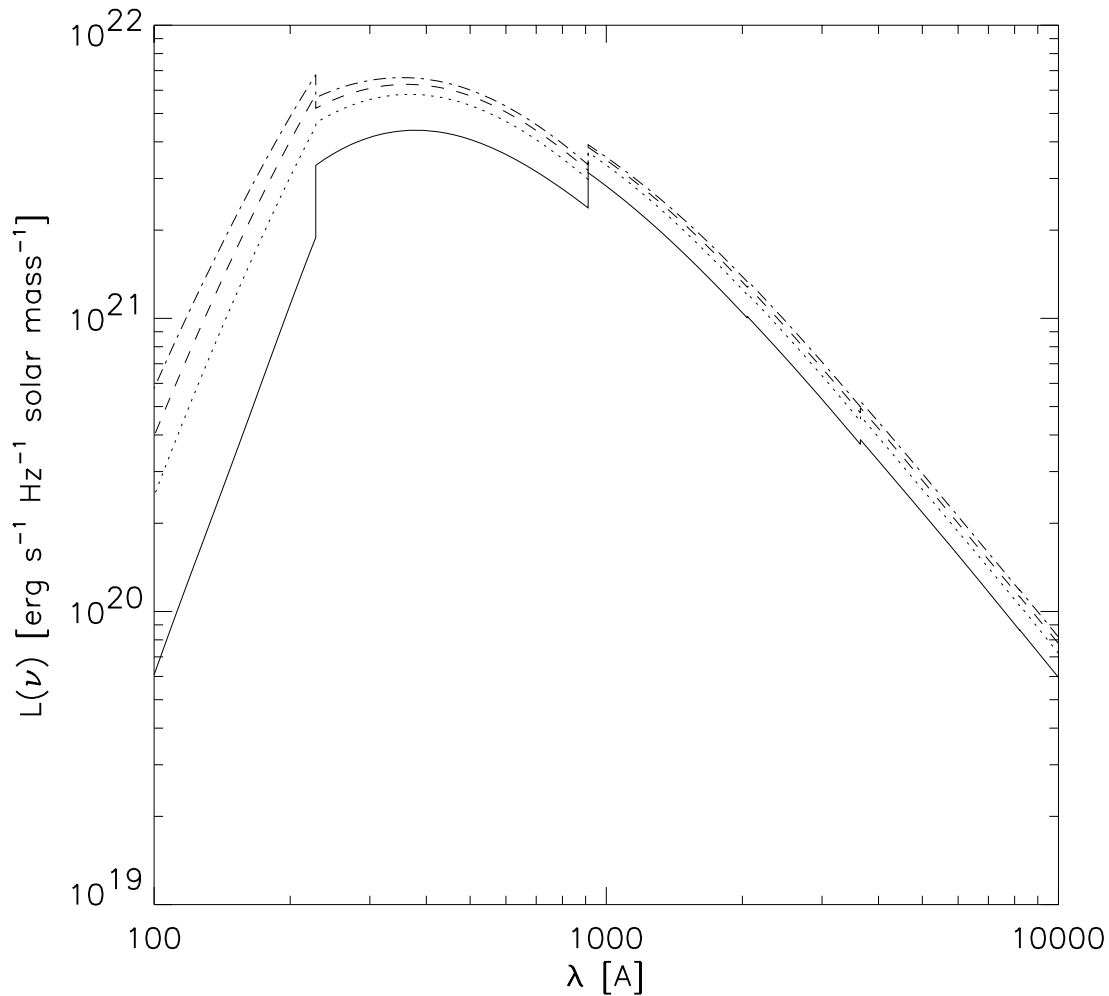
FIG. 3.—Normalized spectral energy distribution in the continuum. Luminosity per unit stellar mass (in ergs s^{-1} Hz^{-1} $M_\odot^{-1}$) vs. wavelength (in Å). *Solid line*: 100 $M_\odot$. *Dotted line*: 300 $M_\odot$. *Dashed line*: 500 $M_\odot$. *Dot-dashed line*: 1000 $M_\odot$. When plotted per unit mass, the spectra admit an almost universal form for $M > 300\ M_\odot$.

per unit mass, L_ν/M, for a 1000 $M_\odot$ star, as given by the dot-dashed line in Figure 3, to be representative for the generic form, and we use it in evaluating the integral in equation (8). The resulting production rates are presented in Table 1. Comparing these rates to the corresponding ones for a Salpeter IMF, as given by Tumlinson & Shull (2000), we find an enhancement in the number of ionizing photons by a factor of 10–20 for H I and He I and by a factor of ~ 75 for He II. We have verified that using L_ν/M for the 300 $M_\odot$

case (Fig. 3, *dotted line*) results in ionization efficiencies that are at most a factor of 2 smaller: 1.2×10^{48} photons s^{-1} $M_\odot^{-1}$ for the ionization of H I, 8.6×10^{47} photons s^{-1} $M_\odot^{-1}$ for He I, and 2.0×10^{47} photons s^{-1} $M_\odot^{-1}$ for He II. By comparing to Table 1, one can see that our choice of the 1000 $M_\odot$ spectrum as being representative for the mass range $1000 > M > 300\ M_\odot$ is well justified.

To illustrate the implications of this result, consider the following zeroth-order estimate for the fraction of baryons that has to be incorporated into stars, f_*, in order to reionize the respective species. Assuming that η ionizing photons are needed per atom ($\eta > 1$ to account for the effect of recombinations), we find for hydrogen

$$f_*(\text{H I}) \simeq \frac{\eta X}{m_{\text{H}}\, \tau_{\text{MS}}\, \dot{N}_{\text{ion}}(\text{H I})} \simeq 10^{-4} \eta_{10}, \qquad (9)$$

where $\eta_{10} = (\eta/10)$ and $\tau_{\text{MS}} \simeq 2 \times 10^6$ yr is the approximate main-sequence lifetime of a very massive star. For helium, one has $f_*(\text{He I}) \simeq 10^{-5} \eta_{10}$ and $f_*(\text{He II}) \simeq 4 \times 10^{-5} \eta_{10}$. The corresponding fractions for a Salpeter IMF are $f_* \sim 10^{-3} \eta_{10}$.

Consequently, if the first stars are indeed characterized by a heavy IMF, the intriguing possibility arises that the rare star-forming clouds, which originate from the high-σ peaks in the primordial density field, might have played an impor-

TABLE 1

PRODUCTION OF IONIZING PHOTONS[a]

Species Particle	E (eV)	$\dot{N}_{\text{ion}}$ (photons s^{-1} $M_\odot^{-1}$)	Y	f_*/η_{10}
H I.............	13.6	1.6×10^{48}	~ 16	1×10^{-4}
He I............	24.6	1.1×10^{48}	~ 14	1×10^{-5}
He II..........	54.4	3.8×10^{47}	~ 75	4×10^{-5}

NOTE.—E is the ionization potential, $\dot{N}_{\text{ion}}$ is the production rate of ionizing photons per unit stellar mass, Y is the ratio of $\dot{N}_{\text{ion}}$ for the cases of a heavy IMF and a Salpeter IMF, and f_* is the required baryon fraction that needs to be converted into stars in order to produce $10\eta_{10}$ ionizing photons per species particle (H I, He I, or He II).

[a] The production rates are calculated for a 1000 $M_\odot$ star. Within a factor of 2, these rates apply to all stars with mass above 300 $M_\odot$.

tant role in the reionization of both hydrogen and helium at high redshifts. Furthermore, helium might have even been reionized before hydrogen. Such a sequence of events would be in marked contrast to the standard scenarios of reionization (e.g., Gnedin & Ostriker 1997; Haiman & Loeb 1997; Gnedin 1998; Ciardi et al. 2000a; Haiman, Abel, & Rees 2000; Miralda-Escudé, Haehnelt, & Rees 2000). Recently, Madau, Haardt, & Rees (1999) have pointed out that the known populations of quasars and star-forming galaxies are not sufficient to account for the required number of ionizing photons at redshifts $z \sim 5$. An early generation of very massive stars could alleviate this problem and contribute a significant part of this unexplained deficit.

4. OBSERVATIONAL SIGNATURE

4.1. *Stellar Spectrum*

Since the first clusters of stars form prior to the epoch of reionization, they are embedded within a neutral IGM. Consequently, the observed flux shortward of the Lyα resonance wavelength, $\lambda_\alpha = 1216$ Å, will be suppressed by the neutral IGM before reionization (Gunn & Peterson 1965) and by the Lyα forest after reionization. The suppression will be complete (as a result of the neutral IGM) for observed wavelengths between $(1 + z_{\mathrm{reion}})\lambda_c$ and $(1 + z_s)\lambda_\alpha$ and partial (as a result of the Lyα forest) at shorter wavelengths (Haiman & Loeb 1999). Here $\lambda_c = 912$ Å is the Lyman limit wavelength, z_s is the source redshift, and z_{reion} is the reionization redshift. The sharp trough of the observed flux at $(1 + z_s)\lambda_\alpha$ can be used to determine unambiguously the redshift of the source, even in the absence of

strong spectral lines. To predict the observed spectrum at wavelengths longer than λ_α, we consider $L(\nu_{\mathrm{em}})$, the monochromatic luminosity per unit stellar mass at the emitted frequency ν_{em}. We again make the assumption that the spectrum for a star of 1000 $M_\odot$ is representative for the mass range $M > 300 M_\odot$. With the flux at the surface of the 1000 $M_\odot$ star being $F(\nu_{\mathrm{em}})$, as shown in Figure 2, one has $L(\nu_{\mathrm{em}}) = 4\pi R^2 F(\nu_{\mathrm{em}})$, where $R \simeq 13.7 R_\odot$ is the stellar radius. The observed flux, unattenuated by the neutral IGM, at a frequency $\nu_{\mathrm{obs}} = \nu_{\mathrm{em}}/(1 + z_s)$ is

$$f(\nu_{\mathrm{obs}}) = \frac{L(\nu_{\mathrm{em}})}{4\pi r^2 (1 + z_s)}, \tag{10}$$

where

$$r = \frac{c}{H_0} \int_0^{z_s} \frac{dz}{\sqrt{\Omega_m (1 + z)^3 + \Omega_\Lambda}}. \tag{11}$$

In Figure 4 we show the predicted spectrum for a cluster at $z_s = 10$, assuming a flat universe with $\Omega_\Lambda = 1 - \Omega_m = 0.7$ and a Hubble constant of $H_0 = 65$ km s^{-1} Mpc^{-1}. We have taken into account the red damping wing of the Gunn-Peterson trough, using the analytical expression given by Miralda-Escudé (1998). In evaluating the optical depth in the vicinity of the Lyα resonance, we assume $z_{\mathrm{reion}} = 7$ and $\Omega_b h = 0.03$, corresponding to a Gunn-Peterson optical depth of $\tau_0(z_s) = 7.4 \times 10^5$. We find that the resulting line shape is not very sensitive to the choice of z_{reion}.

The peak flux is conveniently located in the spectral range between 1 and 5 μm, where *NGST* is expected to reach a photometric sensitivity of ~ 0.1–1 nJy. We plot the
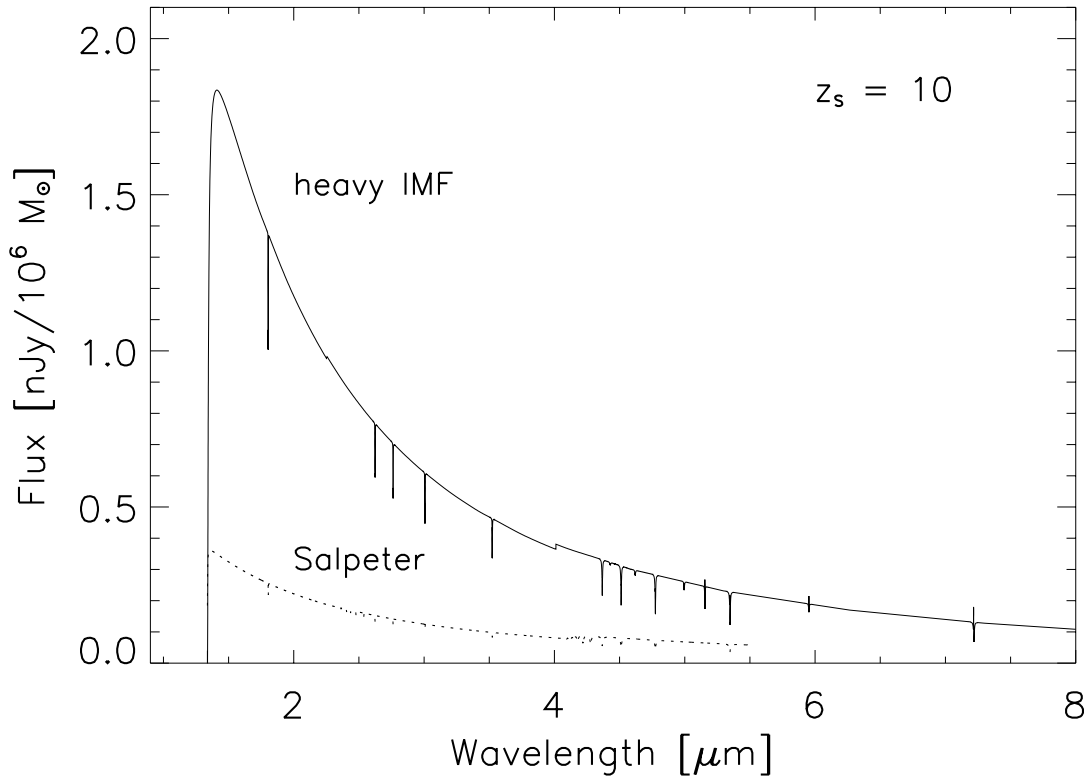

FIG. 4.—Predicted flux from a Population III star cluster at $z_s = 10$. Observed flux (in nJy per $10^6 M_\odot$ of stars) vs. wavelength (in μm). We assume a flat universe with $\Omega_\Lambda = 0.7$ and a Hubble constant of $H_0 = 65$ km s^{-1} Mpc^{-1}. *Solid line:* Case of a heavy IMF. *Dotted line:* Comparison case of a standard Salpeter IMF, where the composite spectrum is taken from Tumlinson & Shull (2000). The cutoff below $\lambda_{\mathrm{obs}} = (1216$ Å$)(1 + z_s) = 1.34 \mu$m is due to complete Gunn-Peterson absorption. It can be seen that for the same amount of total stellar mass, the observable flux is larger by an order of magnitude for stars that are distributed according to a heavy IMF.

flux per $10^6 \, M_\odot$, but it is straightforward to adjust the spectrum to other cases because of the linear scaling with total stellar mass. The composite spectrum of a Salpeter IMF with stellar masses in the range $0.1 \lesssim M/M_\odot \lesssim 100$ has been worked out by Tumlinson & Shull (2000) and is also shown in Figure 4, normalized to the same total stellar mass. In comparing the two spectra, it is evident that the observed flux at any given wavelength is a factor of 5–10 larger for the case calculated with a heavy IMF. The difference in absolute flux, however, will not allow us to discriminate between the two IMFs, since the total stellar mass of the observed system is not known a priori. One instead has to rely on the difference in colors.

For this purpose, we define the ratios F_{12}/F_{23} and F_{23}/F_{45}, where F_{12}, F_{23}, and F_{45} are the integrated fluxes between 1 and 2 μm, 2 and 3 μm, and 4 and 5 μm, respectively. The two colors can then be expressed as a difference in magnitude

$$\Delta m_A = -2.5 \log \frac{F_{12}}{F_{23}} \qquad (12)$$

and

$$\Delta m_B = -2.5 \log \frac{F_{23}}{F_{45}} . \qquad (13)$$

Using the spectra in Figure 4, we find these ratios to be $F_{12}/F_{23} \simeq 2.7$ and $F_{23}/F_{45} \simeq 9.3$ in the case of a heavy IMF and $F_{12}/F_{23} \simeq 2.5$ and $F_{23}/F_{45} \simeq 7.3$ in the case of a Salpeter IMF. In terms of magnitudes, one has

$$\Delta m_A \simeq \begin{cases} -1.1 & \text{for a heavy IMF,} \\ -1.0 & \text{for a Salpeter IMF,} \end{cases}$$

and

$$\Delta m_B \simeq \begin{cases} -2.4 & \text{for a heavy IMF,} \\ -2.1 & \text{for a Salpeter IMF.} \end{cases}$$

Hence, the observed spectrum in the case of a heavy IMF is significantly bluer. Reddening by dust is expected to be weak for the first star clusters (and is already small in some known high-redshift galaxies; see Kudritzki et al. 2000). Moreover, the two colors differentiate between the IMFs in a way that is not degenerate with conventional dust. To see this, we ask, can the presence of dust in the cluster with a heavy IMF cause the two colors to agree simultaneously with those predicted in the Salpeter case? Applying the average extinction curve for the interstellar medium of the Milky Way (e.g., Savage & Mathis 1979), we adjust the amount of dust present in the cluster such that color A is reddened to agree with the prediction for the Salpeter IMF. The corresponding change in color B results in $\Delta m_B \simeq -1.5$, compared to $\Delta m_B \simeq -2.1$ for the Salpeter IMF. Unless one invokes rather contrived properties for the dust, the photometric signature of a heavy IMF therefore cannot masquerade as the one expected from a Salpeter IMF. By measuring these colors, *NGST* might thus be able either to confirm or to exclude the dominance of very massive stars in the early universe.

4.2. *Strong Emission of Recombination Lines*

The hard UV emission from a star cluster with a heavy IMF is likely to be reprocessed by the surrounding inter-

stellar medium and to produce very strong recombination lines of hydrogen and helium. With $\dot{N}_{\rm ion}$ as derived in § 3, the emitted luminosity $L_{\rm line}^{\rm em}$ per unit stellar mass in a particular recombination line can be estimated as follows:

$$L_{\rm line}^{\rm em} = p_{\rm line}^{\rm em} h v \dot{N}_{\rm ion} (1 - p_{\rm cont}^{\rm esc}) p_{\rm line}^{\rm esc} , \qquad (14)$$

where $p_{\rm line}^{\rm em}$ is the probability that a recombination would lead to the emission of a photon in the corresponding line, v is the frequency of the line, and $p_{\rm cont}^{\rm esc}$ and $p_{\rm line}^{\rm esc}$ are the escape probabilities for the ionizing photons and the line photons, respectively. It is natural to assume that the stellar cluster is surrounded by an ionization-bounded H II region, and hence $p_{\rm cont}^{\rm esc}$ is close to zero (Wood & Loeb 2000; Ricotti & Shull 2000). In addition, $p_{\rm line}^{\rm esc}$ is likely to be close to unity in the H II region, as a result of the lack of dust in the ambient metal-free gas. Although the emitted line photons may be scattered by neutral gas, they will diffuse out to the observer and eventually survive if the gas is dust free. Thus, for simplicity, we adopt a value of unity for $p_{\rm line}^{\rm esc}$.

To be concrete, let us consider case B recombination, which yields $p_{\rm line}^{\rm em}$ of about 0.65 and 0.47 for the Lyα and He II $\lambda 1640$ lines, respectively. In arriving at these numbers, we assume an electron temperature of $\sim 3 \times 10^4$ K and an electron density of $\sim 10^2$–10^3 cm^{-3} inside the H II region (see Storey & Hummer 1995). With $\dot{N}_{\rm ion}$ from Table 1, we then obtain $L_{\rm line}^{\rm em} = 1.7 \times 10^{37}$ and 2.2×10^{36} ergs s^{-1} $M_\odot^{-1}$ for the recombination luminosity of Lyα and He II $\lambda 1640$ per embedded stellar mass. A cluster of $10^6 \, M_\odot$ in stars would then produce 4.4 and $0.6 \times 10^9 \, L_\odot$ in the Lyα and He II $\lambda 1640$ lines. Similarly high luminosities would be produced in other recombination lines at longer wavelengths, such as He II $\lambda 4686$ and Hα.

The rest-frame equivalent width of these emission lines measured against the stellar continuum of the embedded cluster at the line wavelengths is given by

$$W_\lambda = \left(\frac{L_{\rm line}^{\rm em}}{L_\lambda} \right) , \qquad (15)$$

where L_λ is the spectral luminosity per unit wavelength of the stars at the line resonance. From Figure 3 we obtain a spectral luminosity per unit frequency $L_v = 2.7 \times 10^{21}$ and 1.8×10^{21} ergs s^{-1} Hz^{-1} $M_\odot^{-1}$ at the corresponding wavelengths. Converting to L_λ, we obtain rest-frame equivalent widths of $W_\lambda = 3100$ and 1100 Å for Lyα and He II $\lambda 1640$, respectively. These extreme emission equivalent widths are more than an order of magnitude larger than the expectation for a normal cluster of hot stars with the same total mass and a Salpeter IMF under the same assumptions concerning the escape probabilities and recombination (e.g., Kudritzki et al. 2000). The equivalent widths are, of course, larger by a factor of $(1 + z_s)$ in the observer frame. Extremely strong recombination lines, such as Lyα and He II $\lambda 1640$, are therefore expected to be an additional spectral signature that is unique to very massive stars in the early universe. Tumlinson & Shull (2000) have discussed the possible observational role of the He II $\lambda 1640$ line in the context of a standard Salpeter IMF.

The He II $\lambda 1640$ line would reach the observer unaffected by the intervening IGM, since its wavelength is longer than that of the Lyα transition that dominates the IGM opacity. However, the Lyα line emitted by the source would be resonantly scattered by the intergalactic H I. At redshifts lower than the reionization redshift, most of the IGM is ionized

and only the blue wing of the line would be suppressed by the Lyα forest. But if the star cluster lies beyond the reionization redshift, the intervening neutral IGM acts as fog and obscures the view of the source at the Lyα wavelength. The line photons emitted by the source scatter until they eventually redshift out of resonance and escape as a result of the Hubble expansion of the surrounding intergalactic H I. As a result, the source creates a faint Lyα halo on the sky (Loeb & Rybicki 1999). For a source at $z_s \sim 10$, the halo occupies an angular radius of $\sim 15''$ and corresponds to a line that is broadened and redshifted by $\sim 10^3$ km s^{-1} relative to the source. The scattered photons are also highly polarized (Rybicki & Loeb 1999). A heavy IMF would make the detection of diffuse Lyα halos around the first star clusters more accessible to future telescopes and would provide an important tool for probing the neutral IGM prior to the epoch of reionization. Observations that focus directly on the bright central source are more straightforward and should show a strong suppression of the Lyα line by the damping wing of the "Gunn-Peterson trough," caused by the IGM scattering (Miralda-Escudé 1998). The very brightest sources might be an exception, in that the H II region they generate in the surrounding IGM might shift the Lyα damping wing and allow a portion of the red wing of the emission line to be observed (Cen & Haiman 2000; Madau & Rees 2000).

5. SUMMARY AND CONCLUSIONS

We have explored the consequences of a possible early generation of very massive, zero-metallicity stars. These stars are almost fully convective and have luminosities close to the Eddington limit and effective temperatures $T_{\rm eff} \sim 10^5$ K that are almost independent of stellar mass. Using a spherically extended, NLTE stellar atmosphere code, we have subsequently constructed the emerging spectra. If normalized by the mass of the star, the spectrum has a generic form, almost independent of mass for $M \gtrsim 300 \, M_\odot$. Based on the photometric colors of the composite spectrum from a cluster of Population III stars, we find that it would be feasible observationally to constrain the primordial IMF with future infrared telescopes such as *NGST* (Fig. 4).

We also investigated the ionizing photon production from these massive stars. Compared to a population of stars with a normal, Salpeter-like IMF, the rate of producing ionizing photons is enhanced by an order of magnitude for H and He I and by a factor of ~ 100 for He II. As a result, the interstellar medium of a star cluster with a heavy IMF is likely to generate extremely strong recombination lines, such as Lyα and He II $\lambda 1640$, with equivalent widths that are larger by at least an order of magnitude compared to a standard IMF.

Very massive Population III stars might have played a significant role in the reionization of the hydrogen and helium in the IGM at high redshifts. The ability to ionize He II efficiently provides an alternative channel for a process that otherwise has to rely on the presence of quasars with their nonthermal spectra. Equally important is the possible contribution of massive stars to the ionizing photon budget at $z \sim 5$, where the known quasars and galaxies are unable to maintain the IGM in an ionized state as long as the IMF is assumed to have the standard form (Madau et al. 1999).

The massive stars considered in this work are likely to end up as black holes (Fryer, Woosley, & Heger 2001). If gamma-ray bursts (GRBs) originate from the collapse of these massive stars, then a heavy IMF will produce a larger abundance of GRBs at high redshifts than previously estimated (Ciardi & Loeb 2000). The bright afterglows of these GRBs would provide an important probe of the IGM at high redshifts (Lamb & Reichart 2000).

REFERENCES

Abel, T., Bryan, G. L., & Norman, M. L. 2000, ApJ, 540, 39
Auer, L. H., & Mihalas, D. 1972, ApJS, 24, 193
Bond, J. R., Arnett, W. D., & Carr, B. J. 1984, ApJ, 280, 825
Bromm, V., Coppi, P. S., & Larson, R. B. 1999, ApJ, 527, L5
———. 2001, ApJ, (astro-ph/0102503)
Carr, B. J., Bond, J. R., & Arnett, W. D. 1984, ApJ, 277, 445
Castor, J. I., Abbott, D. C., & Klein, R. I. 1975, ApJ, 195, 157
Cen, R., & Haiman, Z. 2000, ApJ, 542, L75
Ciardi, B., Ferrara, A., Governato, F., & Jenkins, A. 2000a, MNRAS, 314, 611
Ciardi, B., Ferrara, A., Marri, S., & Raimondo, G. 2000b, MNRAS, submitted (astro-ph/0005181)
Ciardi, B., & Loeb, A. 2000, ApJ, 540, 687
Couchman, H. M. P., & Rees, M. J. 1986, MNRAS, 221, 53
El Eid, M. F., Fricke, K. J., & Ober, W. W. 1983, A&A, 119, 54
Fan, X., et al. 2000, AJ, 120, 1167
Fowler, W. A., & Hoyle, F. 1964, ApJS, 9, 201
Fryer, C. L., Woosley, S. E., & Heger, A. 2001, ApJ, 550, 372
Gabler, R., Gabler, A., Kudritzki, R. P., & Mendez, R. H. 1992, A&A, 265, 656
Gabler, R., Gabler, A., Kudritzki, R. P., Puls, J., & Pauldrach, A. 1989, A&A, 226, 162
Gnedin, N. Y. 1998, MNRAS, 294, 407
Gnedin, N. Y., & Ostriker, J. P. 1997, ApJ, 486, 581
Gunn, J. E., & Peterson, B. A. 1965, ApJ, 142, 1633

Haiman, Z., Abel, T., & Rees, M. J. 2000, ApJ, 534, 11
Haiman, Z., & Loeb, A. 1997, ApJ, 483, 21
———. 1999, ApJ, 519, 479
Husfeld, D., Kudritzki, R. P., Simon, K. P., & Clegg, R. E. S. 1984, A&A, 134, 139
Kippenhahn, R., & Weigert, A. 1990, in Stellar Structure and Evolution (Heidelberg: Springer), 165
Kudritzki, R. P. 1998, in Stellar Astrophysics for the Local Group, VIII Canary Islands Winter School of Astrophysics, ed. A. Aparicio, A. Herrero, & F. Sanchez (Cambridge: Cambridge Univ. Press), 149
———. 2000, in The First Stars, ESO Astrophys. Symp., ed. A. Weiss, T. Abel, & V. Hill (Berlin: Springer), 127
Kudritzki, R. P., et al. 2000, ApJ, 536, 19
Kudritzki, R. P., & Puls, J. 2000, ARA&A, 38, 613
Lamb, D. Q., & Reichart, D. E. 2000, ApJ, 536, 1
Larson, R. B. 1998, MNRAS, 301, 569
Loeb, A. 1998, in ASP Conf. Ser. 133, Science with the NGST (Next Generation Space Telescope), ed. E. Smith & A. Koratkar (San Francisco: ASP), 73
———. 1999, ASP Conf. Ser. 193, The Hy-Redshift Universe: Galaxy Formation and Evolution at High Redshift, ed. A. J. Bunker & W. J. M. van Breugel (San Francisco: ASP), 586
Loeb, A., & Rybicki, G. B. 1999, ApJ, 524, 577
Madau, P., Haardt, F., & Rees, M. J. 1999, ApJ, 514, 648
Madau, P., & Rees, M. J. 2000, ApJ, 542, L69

Miralda-Escudé, J. 1998, ApJ, 501, 15
Miralda-Escudé, J., Haehnelt, M., & Rees, M. J. 2000, ApJ, 530, 1
Motte, F., André, P., & Neri, R. 1998, A&A, 336, 150
Pauldrach, A., Puls, J., & Kudritzki, R. P. 1986, A&A, 164, 86
Rees, M. J. 1999, in AIP Conf. Proc. 470, After the Dark Ages: When
    Galaxies Were Young (the Universe at $2 < z < 5$), ed. S. S. Holt & E.
    Smith (Woodbury: AIP), 13
Ricotti, M., & Shull, J. M. 2000, ApJ, 542, 548

Rybicki, G. B., & Loeb, A. 1999, ApJ, 520, L79
Santolaya-Rey, A. E., Puls, J., & Herrero, A. 1997, A&A, 323, 488
Savage, B. D., & Mathis, J. S. 1979, ARA&A, 17, 73
Schwarzschild, M. 1958, Structure and Evolution of the Stars (Princeton:
    Princeton Univ. Press)
Storey, P. J., & Hummer, D. G. 1995, MNRAS, 272, 41
Tumlinson, J., & Shull, J. M. 2000, ApJ, 528, L65
Wood, K., & Loeb, A. 2000, ApJ, 545, 86